

Lattice dynamics of isotopic alloys with applications to ^{67}Zn Mössbauer spectroscopy

William T. Vetterling and Donald Candela

Lyman Laboratory of Physics, Harvard University, Cambridge, Massachusetts 02138

(Received 14 September 1982; revised manuscript received 24 January 1983)

The "recursion method" is applied to the dynamics of disordered lattices, and is used explicitly to calculate properties of isotopically disordered zinc. The specific heat and atomic motion are calculated for the special case of an isotopically pure lattice and compared to previous experimental and theoretical results. Then Mössbauer-effect calculations for the high-resolution ^{67}Zn isotope are presented, including evaluations of the Mössbauer line shift with temperature, the anisotropic recoil-free fraction, and the Goldanskii-Karyagin effect. In addition, the effect of zero-point motion on the Mössbauer line position and linewidth in isotopically disordered zinc is discussed.

I. INTRODUCTION

Several effects of lattice motion on hyperfine interactions have been predicted for both optical and nuclear transitions.¹⁻⁵ The effects of such motion in disordered systems are of particular interest for the Mössbauer effect. This is because Mössbauer nuclei are frequently either chemically or isotopically different from the nuclei of the host lattice. In the limit of low concentration, this is an impurity problem, while for concentrations of Mössbauer nuclei on the order of unity this becomes the much more difficult problem of a disordered lattice. An extensive review of analytical approaches to both problems has been given by Maradudin *et al.*^{6,7} These calculations have in general involved one or more of the following restrictions: (1) one-dimensional lattices; (2) interactions involving nearest neighbors only; (3) purely isotopic impurities (no change in force constants); (4) cubic symmetry; (5) isolated impurities (with the remainder of the lattice a pure monatomic solid); (6) use of the Debye approximation. Nevertheless, the analytical calculations are important, not only for revealing the physical basis of certain lattice-dynamical effects, but also because of the formidable problems confronting more realistic approaches. The worst of these problems is the enormous number of degrees of freedom that must be treated in the absence of simplifying symmetries. The recursion method of Haydock⁸ and Nex⁹ is valuable for calculations involving disorder or complicated crystal structures (or both). One of its major virtues is the fact that basis states for describing the dynamical motion are chosen in such a way as to reduce the effect of boundary conditions on the solution. Another is its computation-

al efficiency, allowing calculations on systems having thousands of degrees of freedom with modest computing facilities.

We have applied the recursion method to lattice-dynamical problems relevant to the Mössbauer effect, taking a special interest in the isotope ^{67}Zn . This system has the narrowest fractional linewidth of the known Mössbauer resonances, and presents a case in which the contributions of disorder should be, as we shall see, quite observable. In particular, we find that the second-order Doppler shift due to zero-point motion leads to line shifts and line broadening at $T=0$.¹⁰⁻¹³ We show these effects to be small enough to be masked in most instances by chemical isomer shifts. However, if both source and absorber are zinc metal (with perhaps different isotopic compositions), then the linewidth and position should show substantial effects from isotopic disorder. Currently available calculations are constrained with the conditions listed above, most of which do not apply to metallic zinc (or, in fact, to many other cases of practical interest). Therefore, we have applied the recursion method to a simulation of the zinc lattice, based on parameters derived from acoustical and neutron-scattering measurements. All of the properties commonly measured in Mössbauer spectroscopic analysis are easily calculated, and the range of applicability of our method extends well beyond the present problem. In particular, the calculations may be applied to any crystal structure, with arbitrary basis and isotopic composition, at arbitrary temperature, and may be applied with equal ease to isotopic (mass-defect) disorder and to force-constant disorder.

Sections II and III of this paper discuss the recursion method and its application to the Mössbauer ef-

fect. Section IV describes the ^{67}Zn Mössbauer system and a lattice-dynamical model for metallic zinc. We present results of our calculation in Sec. V. Predictions are made for a number of quantities that have yet to be measured in zinc, such as the temperature-dependent recoil-free fraction, the temperature-dependent line shift, and the effects of isotopic disorder on line position and linewidth. In the Appendix we compare the predictions of the recursion method for the zero-point velocity of an isolated impurity with several earlier analytical calculations.

II. THE RECURSION METHOD

The solution of lattice-dynamical problems in the harmonic approximation involves the truncation of a Taylor expansion of the potential energy U at quadratic terms, and discarding linear terms on the basis of lattice stability:

$$U \approx U_0 + \frac{1}{2} \sum_{\alpha, \beta} \sum_{i, j} u_i^\alpha D_{ij}^{\alpha\beta} u_j^\beta.$$

Here u_i^α is the displacement from equilibrium of atom α along the coordinate direction $i = (x, y, z)$, and

$$D_{ij}^{\alpha\beta} = \left. \frac{\partial^2 U}{\partial u_i^\alpha \partial u_j^\beta} \right|_{\{u\}=0}.$$

The equation for the motion of atom α along direction i is

$$m^\alpha \ddot{u}_i^\alpha = - \frac{\partial U}{\partial u_i^\alpha} = - \sum_{\beta, j} D_{ij}^{\alpha\beta} u_j^\beta.$$

The harmonic solutions to this system of equations are found by introducing complex amplitudes v_i^α with

$$u_i^\alpha = \text{Re}(v_i^\alpha e^{i\omega t}),$$

so that

$$m^\alpha \omega^2 v_i^\alpha = \sum_{\beta, j} D_{ij}^{\alpha\beta} v_j^\beta.$$

The resulting eigenvalue problem may be made more symmetrical with respect to the masses m^α by introducing

$$x_i^\alpha \equiv (m^\alpha)^{1/2} v_i^\alpha, \\ \Gamma_{ij}^{\alpha\beta} \equiv (m^\alpha m^\beta)^{-1/2} D_{ij}^{\alpha\beta}.$$

The eigenvalue problem then takes on a simpler form:

$$\sum_{\beta, j} \Gamma_{ij}^{\alpha\beta} x_j^\beta = \omega^2 x_i^\alpha.$$

For a lattice of N atoms, the $3N$ eigenvector solutions may be represented by subscripting them each with their associated value of ω , as $(x_i^\alpha)_\omega$, and we shall take these solutions to be orthonormal:

$$\sum_{\alpha, i} (x_i^\alpha)_\omega (x_i^\alpha)_\sigma = \delta_{\sigma\omega}.$$

It is difficult to carry out the indicated operations for a disordered lattice of reasonable dimensions because the diagonalization of a large matrix is required. However, the recursion method^{8,9} makes possible the efficient numerical evaluation of certain quantities. In this method, one chooses a set of mutually orthogonal basis vectors according to a recursive algorithm, which begins with the choice of a normalized starting vector s_i^α . The recursion method then allows the computation of sums of the form

$$S_{s_i^\alpha}[f] = \sum_{\omega} f(\omega^2) \left[\sum_{\alpha, i} s_i^\alpha (x_i^\alpha)_\omega \right]^2$$

for functions f subject only to modest restrictions.⁹ In this paper we choose starting vectors which involve the motion of a single atom γ along a single direction k ,

$$s_i^\alpha = \delta_{ik} \delta^{\alpha\gamma}$$

and we therefore evaluate sums of the form

$$S_{k\gamma}[f] = \sum_{\omega} f(\omega^2) (x_k^\gamma)_\omega^2.$$

In the next section we show how the lattice dependent quantities used in the Mössbauer analysis may be expressed in this way.

III. MÖSSBAUER EFFECT

The Mössbauer effect is most easily described for a quantum lattice. In terms of the atomic displacements u_i^α and the conjugate momenta $p_i^\alpha = m^\alpha \dot{u}_i^\alpha$ the harmonic Hamiltonian is

$$\mathcal{H} = \sum_{\alpha, i} \frac{(p_i^\alpha)^2}{2m^\alpha} + \sum_{\alpha, i} \sum_{\beta, j} \frac{u_i^\alpha D_{ij}^{\alpha\beta} u_j^\beta}{2}.$$

We introduce the usual annihilation operator for each phonon frequency ω :

$$a_\omega = \sum_{\alpha, i} (x_i^\alpha)_\omega \left[\left(\frac{m^\alpha \omega}{2\hbar} \right)^{1/2} u_i^\alpha + i \left(\frac{1}{2m^\alpha \hbar \omega} \right)^{1/2} p_i^\alpha \right].$$

In terms of these operators the Hamiltonian is

$$\mathcal{H} = \sum_{\omega} \hbar \omega \left(a_\omega^\dagger a_\omega + \frac{1}{2} \right).$$

The quantities of interest in discussing the Mössbauer effect are the thermally averaged expectation values of the squared displacements and velocities of the emitting (or absorbing) Mössbauer nuclei. Inverting the expression for the annihilation operators, we find the thermal average of the mean-square displacement to be given by

$$\langle\langle (u_i^\alpha)^2 \rangle\rangle = \sum_{\omega} (x_i^\alpha)^2_{\omega} \left[\frac{\hbar}{m^\alpha \omega} \right] (\bar{n}_{\omega} + \frac{1}{2}),$$

where \bar{n}_{ω} is the mean number of phonons of frequency ω present at temperature T :

$$\bar{n}_{\omega} = (e^{\beta \hbar \omega} - 1)^{-1},$$

with $\beta = (k_B T)^{-1}$. Similarly

$$\langle\langle (\dot{u}_i^\alpha)^2 \rangle\rangle = \sum_{\omega} (x_i^\alpha)^2_{\omega} \left[\frac{\hbar \omega}{m^\alpha} \right] (\bar{n}_{\omega} + \frac{1}{2}).$$

Both of these thermally averaged quantities assume the form of sums which may be computed using the recursive method discussed earlier,

$$\langle\langle (u_i^\alpha)^2 \rangle\rangle = S_{i\alpha} \left[\frac{\hbar}{m^\alpha \omega} (\bar{n}_{\omega} + \frac{1}{2}) \right],$$

$$\langle\langle (\dot{u}_i^\alpha)^2 \rangle\rangle = S_{i\alpha} \left[\frac{\hbar \omega}{m^\alpha} (\bar{n}_{\omega} + \frac{1}{2}) \right].$$

For the purpose of checking our calculation, it is also desirable to express the heat capacity in a similar form. The two preceding expressions allow the calculation of

$$E = \sum_{i,\alpha} S_{i\alpha} [\hbar \omega (\bar{n}_{\omega} + \frac{1}{2})]$$

which leads to a molar specific heat:

$$C = \frac{R}{N} \sum_{\alpha,i} S_{i\alpha} [(\beta \hbar \omega)^2 \bar{n}_{\omega} (\bar{n}_{\omega} + 1)].$$

The lattice-dependent quantities most relevant to the Mössbauer effect are the second-order Doppler shift and the recoil-free fraction. The former predicts the Doppler dependent thermal line shifts, including the zero-temperature line shift owing to zero-point motion. The latter is important in the determination of integrated line intensity, and its variation with direction leads to the Goldanskii-Karyagin effect.

Provided that anharmonic effects are negligible,^{14,15} the recoil-free fraction for emission in direction i by atom α is

$$f_{i\alpha} = \exp[-4\pi^2 \langle\langle (u_i^\alpha)^2 \rangle\rangle / \lambda^2],$$

where λ is the γ -ray wavelength. Similarly, the

second-order Doppler shift is given by

$$\left[\frac{\Delta \nu}{\nu} \right]_{\alpha} = - \sum_i \frac{\langle\langle (\dot{u}_i^\alpha)^2 \rangle\rangle}{2c^2},$$

where ν is the γ -ray frequency.

IV. METALLIC ZINC

The method will be demonstrated by its application to the resonance of ^{67}Zn Mössbauer nuclei in metallic zinc. This resonance is the narrowest of the known Mössbauer resonances and is the one most likely to show clearly the effects of zero-point motion.^{16,17} Moreover, the zinc-metal lattice is highly anisotropic and should exhibit a large Goldanskii-Karyagin effect.^{18,19}

The ^{67}Zn Mössbauer level at 93.3 keV ($\lambda = 0.13 \text{ \AA}$) is usually reached through the decay of a ^{67}Ga parent with a half-life of 78.3 h. This spin- $\frac{1}{2}$ excited state then decays to the spin- $\frac{5}{2}$ ground state of ^{67}Zn with a half-life of 9.1 μs , leading to a natural resonant Q of about 2×10^{15} (Fig. 1). This corresponds to a natural linewidth of 0.16 $\mu\text{m/s}$ although the observed linewidths will be at least twice this value due to the combined effects of source and absorber. Because of the relatively high recoil energy, the recoil-free fraction is generally less than 2%, and the resonance has been observed only at temperatures below 50 K. In natural form, ^{67}Zn is only present with 4% abundance, but samples enriched to about 90% are available.

Zinc metal has a hexagonal lattice structure with $a_0 = 2.6648 \text{ \AA}$ and $c_0 = 4.9467 \text{ \AA}$.²⁰ The ratio $c_0/a_0 = 1.86$ is rather different than the value for a close-packed hexagonal lattice, 1.63. Several attempts have been made to model the observed acous-

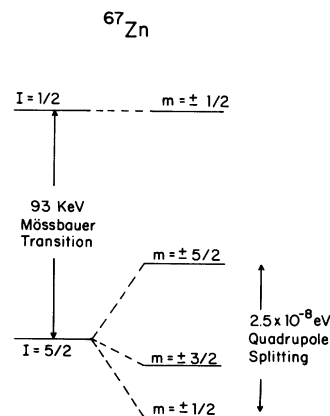


FIG. 1. Energy levels of ^{67}Zn which are relevant to Mössbauer experiments. The total nuclear spin is I , and the projection of this spin along the c axis is m .

tic properties and phonon dispersion relation (from neutron scattering).²¹⁻²⁸ Theories which do not account for force constants between each atom and an adequate number of neighbors, or for a sufficiently general form of interaction, have generally had limited success. The modified axially symmetric (MAS) model of DeWames *et al.*^{27,28} has perhaps been the most successful, and also fits conveniently within the structure of our calculation. The model derived from a simpler axially symmetric model²⁹ which characterized the bond between each pair α, β of atoms by a restoring force $C_1(\alpha, \beta)$ for bond stretching, and a restoring force $C_B(\alpha, \beta)$ for bond bending. In terms of these constants, the potential at site α is given by

$$V_\alpha = \frac{1}{2} \sum_{\beta} \{ C_1(\alpha, \beta) [\hat{n}^{\alpha\beta} \cdot (\bar{u}^\beta - \bar{u}^\alpha)]^2 + C_B(\alpha, \beta) [\hat{n}^{\alpha\beta} \times (\bar{u}^\beta - \bar{u}^\alpha)]^2 \},$$

where $\hat{n}^{\alpha\beta}$ is a unit vector pointing from α to β . This potential may be used to derive the dynamical matrix

$$D_{ij}^{\alpha\beta} = (1 - \delta^{\alpha\beta}) (-K^{\alpha\beta} n_i^{\alpha\beta} n_j^{\alpha\beta} - \delta_{ij} C_B^{\alpha\beta}) + \delta^{\alpha\beta} \sum_{\gamma} (K^{\alpha\gamma} n_i^{\alpha\gamma} n_j^{\alpha\gamma} + \delta_{ij} C_B^{\alpha\gamma})$$

with $K^{\alpha\beta} = C_1^{\alpha\beta} - C_B^{\alpha\beta}$. The MAS model differs in that two bending constants, C_{Bxy} and C_{Bz} , are used. The second is used only in the term $\delta_{ij} C_B$ when $i = 3$. No rigorous justification for this substitution is given but it leads to a more accurate description of the observed phonon dispersion relation. The values of K , C_{Bxy} , and C_{Bz} for the first six nearest-neighbor shells (38 neighbors) have been determined on the basis of neutron scattering data.²⁷

We have used this model along with randomly distributed masses in the desired isotopic proportions to create simulated lattices for calculations of Mössbauer effect quantities. Typically, these lattices had $8 \times 8 \times 5$ unit cells, giving almost 2000 degrees of freedom. Previous calculations of the specific heat²⁷ and the density of states²⁸ for the MAS model²⁷ were used to check our calculation. These results are included in the next section.

V. RESULTS

Density of states. The eigenfrequency sums

$$S_{k\gamma}[f] = \sum_{\omega} f(\omega^2) (x_k^\gamma)^2$$

that we evaluate in this paper clearly focus upon the local environment of the Mössbauer nucleus because the function $f(\omega^2)$ is weighted for each mode fre-

quency by the motional amplitude of the nucleus in that mode. An important example is the so-called "local density of states,"

$$n_i^\alpha(\nu) = \sum_{\omega} \delta(\nu - \omega/2\pi) (x_i^\alpha)^2.$$

In the special case of a uniform lattice, the local density of states (when averaged over $i = x, y, z$) is equal to the usual full phonon density of states. (In a disordered system, on the other hand, the local density of states varies from site to site.) A graph of the local density of states we compute for a pure zinc lattice is given in Fig. 2(a). We have used the smoothing prescription of Ref. 9. This function may be compared with the full density of states for the MAS model²⁷ of zinc, Fig. 2(b),²⁸ and to the full density of states for another zinc model, Fig. 2(c).³⁰ The densities of states in Figs. 2(b) and 2(c) were both computed using k -space sampling techniques. Our calculation would agree in detail with Fig. 2(b) if it were possible to carry it out to much higher precision, since both analyses are based on the MAS model.²⁷

Specific heat. The originators of the MAS model verified that it made accurate predictions for the specific heat.²⁷ Thus a calculation of this quantity within the framework of the recursion method can serve as a test, both for the accuracy of the method and for the correctness of our implementation of the

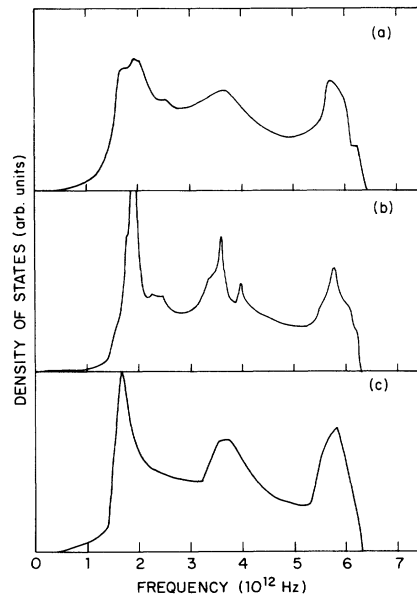


FIG. 2. Phonon densities of states for metallic zinc. (a) Recursion method applied to the MAS model (this paper). (b) Root-sampling method for the MAS model (Ref. 28). (c) Root-sampling method applied to an earlier model (Ref. 30).

MAS model. The computed specific heat as a function of temperature is shown in Fig. 3, and it is compared there with experimental data.³¹⁻³³ The agreement is quite satisfactory.

Mean-square displacement. Figure 4 shows the calculated mean-square displacement of zinc atoms as a function of temperature. For zinc, $\langle z^2 \rangle$ is different than $\langle x^2 \rangle = \langle y^2 \rangle$ so these are drawn separately. Values given by Barron and Munn³⁴ are in agreement with these results but are not independent. Their values of $\langle x^2 \rangle$, $\langle y^2 \rangle$ were also determined by applying the MAS model, albeit with different numerical techniques appropriate to ideal lattices. They then chose $\langle z^2 \rangle$ for consistency with thermodynamic data. Also plotted in Fig. 4 are two low-temperature experimental determinations of mean-square displacements^{35,36} derived mainly from x-ray data. A discussion of other determinations of these displacements and their interpretation is provided in Refs. 37 and 38. Related measurements of the mean-square nuclear displacements of ⁵⁷Fe impurities in zinc, performed via the Mössbauer effect, have been reported^{39,40} and are in general agreement with our calculation.

The calculated mean-square displacements can be used also to determine the recoil-free fraction f as a function of temperature, and of direction with respect to the crystal c axis. For a harmonic hexagonal lattice, f is fully characterized by its values f_z and f_x for emission along or perpendicular to the c axis. In an arbitrary direction \hat{n} , f is given by

$$f = \exp[-\langle (\hat{n} \cdot \vec{x})^2 \rangle / \lambda^2] \\ = f_x (f_z / f_x)^{\cos^2 \theta},$$

where θ is the angle between \hat{n} and the c axis. At $T=0$, and for a natural ⁶⁷Zn lattice, $f_x = 1.1 \times 10^{-2}$ and $f_z = 3.3 \times 10^{-4}$. The recoil-free fraction is

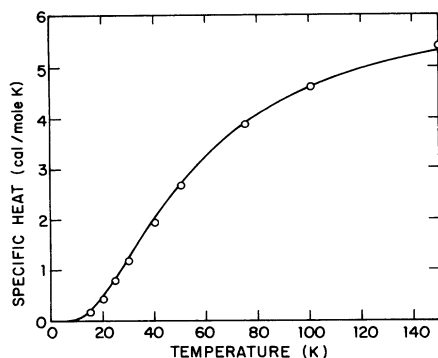


FIG. 3. Specific heat of zinc, calculated from the recursion method (solid line). Experimental specific heat from Ref. 32 (circles).

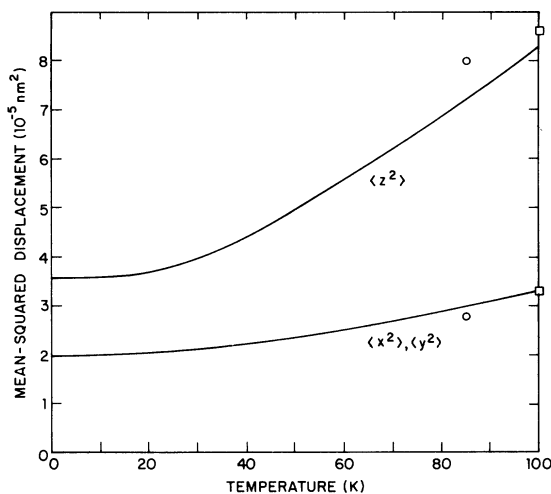


FIG. 4. Mean-squared atomic displacement in zinc, calculated from the recursion method (solid lines). $\langle z^2 \rangle$ is the displacement along the c axis. The mean-squared displacement deduced from x-ray experiments is shown by circles (Ref. 36) and squares (Ref. 35).

therefore highly suppressed for emission along the c axis, a fact first noted by Pound and Rebka.¹² The results may be used to evaluate the Goldanskii-Karyagin effect for zinc metal powder as a function of temperature. The ⁶⁷Zn ground state, as indicated in Fig. 1, has spin $\frac{5}{2}$, and is split into three sublevels by the electric field gradient internal to the zinc-metal lattice. The first nuclear excited state has spin $\frac{1}{2}$ and remains unsplit. The emission spectrum thereby splits into three components of equal integrated intensity, each radiated with a different angular pattern with respect to the c axis.⁴¹ The radiation pattern of recoil-free photons is modified further by the anisotropy of the recoil-free fraction, yielding the angular emission patterns shown in Fig. 5. The $\pm \frac{1}{2} \rightarrow \pm \frac{3}{2}$ and the $\pm \frac{1}{2} \rightarrow \pm \frac{1}{2}$ lines are more strongly localized along the c axis and are reduced in integrated intensity with respect to the $\pm \frac{1}{2} \rightarrow \pm \frac{5}{2}$ line as a result of the anisotropic f value. When averaged over solid angle, we obtain relative line intensities shown in Fig. 6 for $(\pm \frac{5}{2}, \pm \frac{3}{2}, \pm \frac{1}{2})$. These relative intensities would be 1:1:1 at all temperatures in the absence of anisotropy in the mean-square displacements. Experimental measurements⁴² at 4.2 K, where we predict relative intensities of (1.00):(0.87):(0.65), give values of $(1.00):(0.89 \pm 0.18):(0.79 \pm 0.23)$. Further data are clearly needed to provide a definitive test. We also calculate that the line intensities are 55%, 48%, and 36%, respectively, of what they would be if radiation in the xy plane only were used (in an experiment with an oriented single crystal).

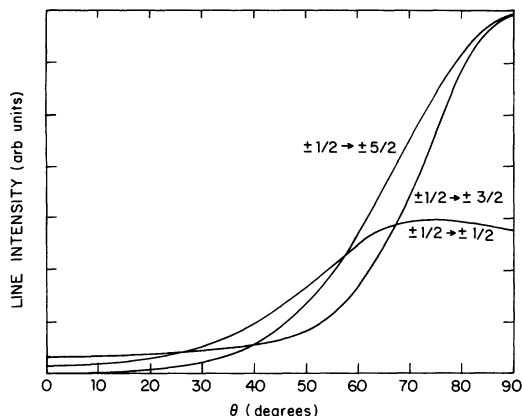


FIG. 5. Predicted intensity for the three components of the Mössbauer line, as a function of the angle θ between the emission direction and the c axis. The curves are labeled by the change in the magnetic quantum number m .

Mean-square velocity. Our numerical methods also allow the calculation of the mean-square atomic velocity $\langle v^2 \rangle$ as a function of temperature. Figure 7 shows the resulting prediction for the second-order Doppler contribution to the temperature shift of the Zn(^{67}Ga) Mössbauer spectrum. Experimental data for this quantity are not yet available.

A more difficult calculation is the determination of the effects of isotopic disorder on the Mössbauer line properties. We treat two examples here: (1) The difference in the second-order Doppler shift from zero-point motion due to differences in isotopic composition of source and absorber; (2) broadening of the Mössbauer lines due to site-to-site variations in zero-point motion in an isotopically disordered lattice. We believe the recursion-method calculation is the first to give reliable results for these two effects, which we treat in turn below.

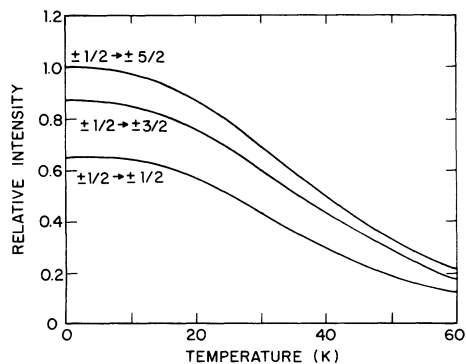


FIG. 6. Temperature dependence of the intensities of the three components of the Mössbauer line, for a powder sample of metallic zinc. The intensities have been normalized to that of the $m = \pm \frac{1}{2} \rightarrow m = \pm \frac{5}{2}$ line at $T=0$.

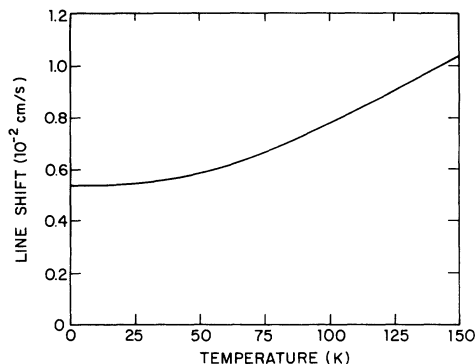


FIG. 7. Predicted shift in the position of the ^{67}Zn Mössbauer line, for a metallic zinc host, owing to the second-order Doppler effect.

Line shifts. Even in the $T \rightarrow 0$ limit, a contribution of the second-order Doppler term to the line position remains due to zero-point motion. Using the Debye approximation, this shift may be estimated to be roughly $\Delta\nu/\nu = -1.5 \times 10^{-13}$ or about 300 natural linewidths. Consequently, it has been considered as a possible contribution to observed isomer shifts.¹⁷ On the other hand, one cannot measure the absolute shift, only its variation from one lattice to another. The calculations discussed in the Appendix all suggest that this variation is far smaller than the shift itself. Although corrections have been made in some cases for the shift^{17,43} its presence has not been confirmed experimentally. The principal obstacle to doing so is the fact that chemically inequivalent sources and absorbers also exhibit line shifts due, for example, to differing electrostatic contact interactions between the electrons and the nucleus. These are evidently larger in most cases than the zero-point shift.^{17,44}

One possible solution is to use a source and absorber which are chemically identical and differ only in isotopic composition.^{45,46} For example, we consider here the shift which would be observed between a source lattice of natural zinc and a commercially available⁴⁷ zinc absorber enriched to about 90% in ^{67}Zn . The zero-point shift in this case is expected to be quite small, but relatively uninfluenced by chemical shifts. Our recursion-method calculation predicts a relative line shift for this source-absorber combination of $0.0266(10) \mu\text{m/s}$. This is 17% of the natural linewidth (8% of the observable width), and so should be readily measurable. An experimental test is underway in our laboratory. Data of this type are available for ZnO, but apparently without sufficient precision in the isomer shift. The two available measurements^{46,48} differ in both sign and magnitude. We have not attempted a recursion-method calculation for ZnO, a substance

for which the additional complication of long-range interactions will have to be considered. In the Appendix, we compare our recursion-method results for the zero-point shift with the predictions of several analytical calculations. These analytical methods are not applicable to the full isotopic alloy problem, so the comparison is done for the case of an isolated ^{67}Zn impurity in a host lattice with zinc force constants, but with variable atomic mass. All of the calculations agree on the sign and general size of the shift, for this somewhat artificial case.

Line broadening. In a lattice with disorder, such as an isotopic mixture, the various lattice sites are not equivalent and one can expect a distribution of mean-square velocities. The variation in resulting Doppler shifts will lead to line broadening even for an otherwise perfect crystal at zero temperature, as was first pointed out by Snyder and Wick.⁴⁹ Our recursion-method simulations of natural and enriched zinc give explicit predictions for this broadening effect, which would be absent in pure ^{67}Zn . We predict an excess linewidth of 0.0094(8) $\mu\text{m/s}$ for natural zinc, and an excess linewidth of 0.0027(2) $\mu\text{m/s}$ for zinc enriched to 90% ^{67}Zn . An experiment would observe the combined effects of source and absorber, but the increase over natural linewidth is only 6% for a natural source and absorber. This effect is important, however, because it places foreseeable limits on the resolution that may be achieved for isotopically mixed systems. The order of magnitude of this limit is $|\Delta\nu/\nu| = 10^{-16}$ and, since practical Mössbauer γ -ray energies are ≤ 100 keV, suggests a limiting linewidth of several hundred hertz (the excess linewidth is 700 Hz in natural zinc). Similar limits are expected from electromagnetic interactions within the solid, such as the dipole-dipole interactions. Attempts have been made to observe the Mössbauer effect with long-lived isomeric states of Ag^{107} and Ag^{109} (with 44.3 and 39.6 s half-life, respectively).⁵⁰⁻⁵² Our calculation suggests that the site-to-site variations of zero-point motion in natural silver will broaden the line to about 10^5 times its natural width, rendering the resonance unobservable.

VI. CONCLUSION

This paper presents a method for determining the dynamical properties of atoms in three-dimensional lattices of arbitrary crystal structure. The method can treat disorder in either the masses or the force constants, the sole restriction being the availability of an adequate harmonic model for the system. The case of zinc metal, a highly anisotropic hexagonal crystal, has been investigated and results are provided for the temperature dependence of the second-

order Doppler induced isomer shift, the recoil-free fraction, and the Goldanskii-Karyagin effect. We have predicted a measurable line shift between a natural zinc source and an enriched zinc absorber, owing to differences in zero-point motion. The achievable Mössbauer energy resolution in isotopically mixed systems is seen to be limited by isotopic disorder. Existing data on the motion of ^{57}Fe in zinc and on the isomer shift of ^{67}Zn atoms in a copper lattice (with respect to a zinc-metal absorber) should also provide interesting tests for our calculational method. In these cases, both the masses and the force constants are modified at the sites of the Mössbauer nuclei.

ACKNOWLEDGMENTS

We would like to thank Professor R. V. Pound for discussions regarding these calculations. This work was done with the support of the National Science Foundation under Grant No. DMR79-07023.

APPENDIX

In this Appendix we evaluate the results of several analytical approaches to the problem of impurity zero-point velocity, in order to compare them with our numerical calculations. We stress that these analytical methods are restricted to the isolated impurity problem, unlike our recursion calculation. Further information on these methods may be found in the reviews of Maradudin *et al.*^{6,7} In each case, we have evaluated the mean-square zero-point velo-

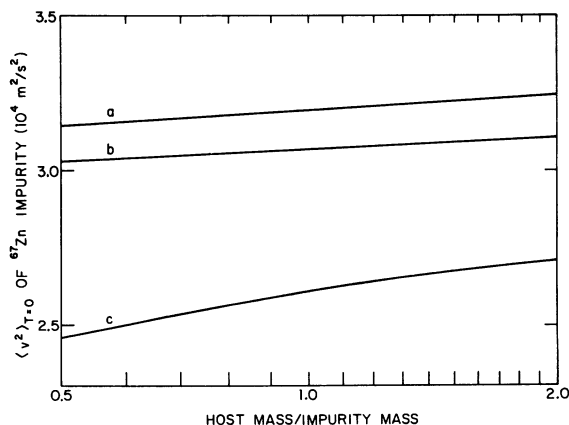


FIG. 8. Predictions of various models for the mean-square velocity of a ^{67}Zn impurity, as a function of the host-lattice atomic mass. See the Appendix for details. (a) Recursion method applied to the MAS model (our calculation). (b) Perturbative result of Lipkin, and result of Maradudin *et al.* The two results, which are both based on the Debye model, are indistinguishable on the scale of this graph. (c) One-dimensional lattice calculation.

city for an impurity of mass M' in a perfect lattice of atoms with mass M , using force constants appropriate to metallic zinc. Most of the models predict line shifts proportional to the Debye temperature Θ_D . As we have noted, metallic zinc is particularly poorly described by the Debye approximation. Various methods of measuring Θ_D have led to values varying by more than 100 K.³⁷ For computational purposes we have used $\Theta_D = 220$ K, which is perhaps the most favorable value for agreement with our more realistic calculations.

The results are presented in Fig. 8 for the case in which the impurity is ^{67}Zn and the mass M of the

host-lattice atoms varies. Except for the case in which the host is another isotope of zinc, these results do not pertain to actual experiments. Nevertheless, this provides an effective way to compare the various methods.

One-dimensional lattices. The greatest amount of progress with lattice impurity dynamics has been achieved in calculations for monatomic and diatomic one-dimensional lattices.⁵³ The lattice is usually assumed to be bound by nearest-neighbor harmonic interactions. For the monatomic case, we are able to write the mean-squared velocity of an isolated impurity for the mode of frequency ω as⁵⁴

$$\langle v^2 \rangle_\omega = \left[\frac{1}{NM} \right] \frac{\hbar\omega \coth(\hbar\omega/2kT)}{1 + \epsilon^2 \tan^2(\phi_\omega/2) - (\epsilon/N)[1 + \tan^2(\phi_\omega/2)]},$$

where N is the number of atoms in the chain, $\epsilon = (M - M')/M$, and ϕ_ω is defined implicitly by

$$\tan(N\phi_\omega/2) = \epsilon \tan(\phi_\omega/2).$$

The net impurity velocity may be evaluated by approximating the resulting sum over ω as an integral which can be evaluated analytically. In the low-temperature limit, the expression becomes⁵⁵

$$\langle v^2 \rangle = \begin{cases} \frac{\hbar\omega_L}{\pi M} \left[\frac{1}{1 - \epsilon^2} - \frac{|\epsilon|}{(1 - \epsilon^2)^{3/2}} \tan^{-1} \frac{(1 - \epsilon^2)^{1/2}}{|\epsilon|} \right] & \text{for } 0 < \epsilon^2 < 1 \\ \frac{\hbar\omega_L}{\pi M} \left[\frac{|\epsilon|}{(\epsilon^2 - 1)^{3/2}} \tanh^{-1} \left[\frac{(\epsilon^2 - 1)^{1/2}}{|\epsilon|} \right] - \frac{1}{\epsilon^2 - 1} \right] & \text{for } \epsilon^2 > 1, \end{cases}$$

where $\omega_L = (4\gamma/M)^{1/2}$ is the maximum frequency in the acoustic spectrum of the unperturbed lattice, and γ is the nearest-neighbor force constant. To these results must be added the contribution from a localized mode⁵⁶⁻⁵⁸ if $0 < \epsilon < 1$. In this case, the highest mode in the acoustic band separates off from the others and makes a separate resonance above the highest frequency in the spectrum, ω_L . The solution makes a contribution to $\langle v^2 \rangle$ of

$$\Delta \langle v^2 \rangle = \frac{\hbar\omega_L}{M} \left[\epsilon \coth \left[\frac{\hbar\omega_L}{2kT} \frac{1}{(1 - \epsilon^2)^{1/2}} \right] \right] (1 - \epsilon^2)^{-3/2}.$$

In the Debye model for three-dimensional lattices, the highest lattice frequency is $\omega_L = k\Theta_D/\hbar$. For comparison with three-dimensional models, we have used this value for ω_L , and in addition we have multiplied the mean-square velocity by three to account for the extra degrees of freedom in three dimensions.

Three dimensions. While one-dimensional calculations give some insight into the isolated impurity problem, they do not represent realistic models of the usual lattice-dynamical problem. Their value lies in the fact that the equivalent three-dimensional problem becomes intractable when applied to systems of any complexity.

Lipkin has applied perturbation theory to arrive at a result for lattices of arbitrary dimensionality.⁵⁹ By examining the effect on the motion of one atom by the simultaneous change in the masses of all oth-

er atoms in the lattice (without changing the force constants), he calculates the first-order shift in zero-point velocity in terms of the spectrum of the unperturbed lattice. If his result is evaluated for a Debye spectrum, we find

$$\langle v^2 \rangle = \left[\frac{9}{8} \frac{k\Theta_D}{M'} \left(\frac{M}{M'} \right)^{1/2} \right]^2 (1 + 0.019\epsilon).$$

Note that the term in square brackets is independent of ϵ because $\Theta_D \propto M^{-1/2}$. The only barrier to using this calculation to obtain an accurate estimate of the zero-point shift in zinc, is the necessity of approximating a host lattice of varying isotopic composition by a uniform host of varying mass.

Maradudin *et al.* have given a nonperturbative calculation for three dimensions (restricted, howev-

er, to isotopic impurities in a monatomic cubic lattice).⁵⁵ Following from the very general result that

$$\langle v^2 \rangle = \frac{2}{M'} \frac{d}{d\epsilon} [\Delta F(\epsilon, T)],$$

where $\Delta F(\epsilon, T)$ is the change in the free energy of the crystal at temperature T owing to the introduction of the impurity, it is possible to evaluate the mean-squared impurity velocity. In the low-temperature limit, the result becomes

$$\langle v^2 \rangle = \frac{3\hbar\omega_L}{\pi M'} \int_0^\infty \frac{2f^2 G(f) + f^3 G'(f)}{[(1 - \epsilon f^2 G(f))^2]} df,$$

where

$$G(f) = \int_0^1 \frac{P(x) dx}{f^2 + x^2},$$

$$P(x) = \omega_L g(\omega_L x),$$

and $g(\omega)$ is the normalized frequency spectrum of the unperturbed host. Provided that the density of

states can be found by other means, the integrals indicated can be evaluated numerically. Zinc, of course, is not cubic so this calculation is not directly applicable. As an approximation we have used these formulas and a Debye spectrum to calculate the results shown in Fig. 8. It is interesting to note that the zero-point shift estimated in this way is indistinguishable from that predicted by Lipkin's perturbation theory for a Debye model.

The results in this Appendix represent only a fraction of the progress achieved with such calculations. Other results for three-dimensional lattices dealing particularly with localized modes at the impurity, were derived by Dawber and Elliott⁶⁰ using the Green's-function techniques of Lifšic.⁵⁶ These calculations were for isotopic impurities in a Debye lattice. Results for more highly disordered three-dimensional lattices have been found by Weiss and Maradudin,⁶¹ and applied to two-component simple cubic lattices with nearest-neighbor interactions. Further extensions of the techniques above are reviewed by Maradudin *et al.*⁷

- ¹G. F. Imbusch, W. M. Yen, A. L. Schawlow, G. E. Devlin, and J. P. Remeika, *Phys. Rev.* **136**, A481 (1964).
²J. Grabmaier, S. Hufner, E. Orlich, and J. Pelzl, *Phys. Lett.* **24A**, 680 (1967).
³J. Pelzl, P. Abt, and S. Hufner, *Z. Phys.* **248**, 150 (1971).
⁴G. K. Shenoy, F. E. Wagner, and G. M. Kalvius, in *Mössbauer Isomer Shifts*, edited by G. K. Shenoy and F. E. Wagner (North-Holland, Amsterdam, 1978), p. 101ff.
⁵F. S. Ham, *J. Phys. (Paris) Colloq.* **35**, C6-121 (1974).
⁶A. A. Maradudin, in *Solid State Physics*, edited by F. Seitz and D. Turnbull (Academic, New York, 1966) Vols. 18 and 19.
⁷A. A. Maradudin, E. W. Montroll, G. H. Weiss, and I. P. Ipatova, in *Solid States Physics*, edited by H. Ehrenreich, F. Seitz, and D. Turnbull (Academic Press, New York, 1971), Vol. 35.
⁸R. Haydock, in *Solid State Physics*, Ref. 7, pp. 215-294.
⁹C. M. N. Nex, *J. Phys. A* **11**, 653 (1978).
¹⁰R. V. Pound and G. A. Rebka, Jr., *Phys. Rev. Lett.* **4**, 274 (1960).
¹¹B. D. Josephson, *Phys. Rev. Lett.* **4**, 341 (1960).
¹²R. V. Pound and G. A. Rebka, Jr., *Phys. Rev. Lett.* **4**, 397 (1960).
¹³J. van Kranendonk, in *Proceedings of the VII International Conference on Low Temperature Physics*, edited by G. M. Graham and A. C. Hollis-Hallett (University of Toronto Press, Toronto, 1961), pp. 9-20.
¹⁴A. A. Maradudin and P. A. Flinn, *Phys. Rev.* **129**, 2529 (1963).
¹⁵T. H. K. Barron, A. J. Leadbetter, J. A. Morrison, and L. S. Salter, *Acta Crystallogr.* **20**, 125 (1966).
¹⁶W. T. Vetterling, in *Mössbauer Spectroscopy and Its*

- Chemical Applications*, edited by John G. Stevens and Gopal K. Shenoy (American Chemical Society, Washington, 1981), pp. 329-345.
¹⁷D. Griesinger, R. V. Pound, and W. Vetterling, *Phys. Rev. B* **15**, 3291 (1977).
¹⁸S. V. Karyagin, *Fiz. Tverd. Tela (Leningrad)* **8**, 1739, (1966) [*Sov. Phys.—Solid State* **8**, 1387 (1966)].
¹⁹V. Karyagin, *Fiz. Tverd. Tela (Leningrad)* **9**, 2514 (1967) [*Sov. Phys.—Solid State* **9**, 1979 (1968)].
²⁰R. W. G. Wyckoff, *Crystal Structures*, 2nd ed. (Wiley and Sons, New York, 1963), Vol. 1.
²¹R. E. Joynson, *Phys. Rev.* **94**, 851 (1954).
²²G. Gilat, G. Rizzi, and G. Cubiotti, *Phys. Rev.* **185**, 971 (1969).
²³S. Prakash and S. K. Joshi, *Phys. Rev. B* **1**, 1468 (1970).
²⁴G. Bose, B. B. Tripathi, and H. C. Gupta, *J. Phys. Soc. Jpn.* **34**, 1006 (1973).
²⁵J. Panitz, P. H. Cutler, and W. F. King III, *J. Phys. F* **4**, L106 (1974).
²⁶S. K. Mishra and S. S. Kushwaha, *Nuovo Cimento* **46B**, 380 (1978).
²⁷R. E. DeWames, T. Wolfram, and G. W. Lehman, *Phys. Rev.* **138**, A717 (1965).
²⁸L. J. Raubenheimer and G. Gilat, *Phys. Rev.* **157**, 586 (1967).
²⁹G. W. Lehman, T. Wolfram, and R. E. DeWames, *Phys. Rev.* **128**, 1593 (1962).
³⁰J. A. Young and J. U. Koppel, *Phys. Rev.* **134**, A1476 (1964).
³¹P. L. Smith, *Philos. Mag.* **46**, 744 (1955).
³²R. Hultgren, R. Orr, P. Anderson, and K. Kelley, *Selected Values of Thermodynamic Properties of Metals and Alloys*, (Wiley, New York, 1963), p. 318.

- ³³D. L. Martin, *Phys. Rev.* **167**, 640 (1968).
- ³⁴T. H. K. Barron and R. W. Munn, *Acta Crystallogr.* **22**, 170 (1967).
- ³⁵G. E. M. Jauncey and W. A. Bruce, *Phys. Rev.* **51**, 1067 (1937).
- ³⁶E. O. Wollan and G. G. Harvey, *Phys. Rev.* **51**, 1054 (1937).
- ³⁷E. F. Skelton and J. L. Katz, *Phys. Rev.* **171**, 801 (1968).
- ³⁸E. Rossmannith, *Acta Crystallogr. Ser. A* **36**, 416 (1980).
- ³⁹R. M. Housley and R. H. Nussbaum, *Phys. Rev.* **138**, A753 (1965).
- ⁴⁰W. Kundig, K. Ando, and H. Bommel, *Phys. Rev.* **139**, A889 (1965).
- ⁴¹H. Frauenfelder, D. E. Nagle, R. D. Taylor, D. R. F. Cochran, and W. M. Visscher, *Phys. Rev.* **126**, 1065 (1962).
- ⁴²W. Potzel, A. Forster, and G. M. Kalvius, *Phys. Lett.* **67A**, 421 (1978).
- ⁴³L. Pfeiffer and T. Kovacs, *Phys. Rev. B* **23**, 5725 (1981).
- ⁴⁴A. Forster, W. Potzel, and G. M. Kalvius, *Z. Phys. B* **37**, 209 (1980).
- ⁴⁵P. P. Craig, D. E. Nagle, and D. R. F. Cochran, *Phys. Rev. Lett.* **4**, 561 (1960).
- ⁴⁶H. de Waard and G. J. Perlow, *Phys. Rev. Lett.* **24**, 566 (1970).
- ⁴⁷Enriched zinc (composition: 89.7 at. % ⁶⁷Zn, 4.5 at. % ⁶⁶Zn, 4.2 at. % ⁶⁸Zn, 1.7 at. % ⁶⁴Zn) from Oak Ridge National Laboratory.
- ⁴⁸A. I. Beskronny, N. A. Lebedev, and Yu M. Ostanovich (unpublished). Joint Institute for Nuclear Research (Dubna, USSR) preprint P14-5958, 1971.
- ⁴⁹H. S. Snyder and G. C. Wick, *Phys. Rev.* **120**, 128 (1960).
- ⁵⁰G. E. Bizina, A. G. Beda, N. A. Burgov, and A. V. Davydov, *Zh. Eksp. Teor. Fiz.* **45**, 1408 (1963) [*Sov. Phys.—JETP* **18**, 973 (1964)].
- ⁵¹B. G. Alpatov, A. G. Beda, G. E. Bizina, A. V. Davydov, and M. M. Korotokov, in *Proceedings of the International Conference on Mössbauer Spectroscopy*, Bucharest, Romania, 1977 (unpublished), p. 43.
- ⁵²W. Wildner and U. Gonser, *J. Phys. (Paris) Colloq.* **3**, C2-47 (1979).
- ⁵³J. Mahanty, A. A. Maradudin, and G. H. Weiss, *Prog. Theor. Phys.* **20**, 369 (1958).
- ⁵⁴R. F. Wallis and A. A. Maradudin, *Prog. Theor. Phys.* **24**, 1055 (1960).
- ⁵⁵A. A. Maradudin, P. A. Flinn, and S. Ruby, *Phys. Rev.* **126**, 9 (1962).
- ⁵⁶M. Liffšic, *Nuovo Cimento Suppl.* **3**, 716 (1956).
- ⁵⁷E. W. Montroll and R. B. Potts, *Phys. Rev.* **100**, 525 (1955).
- ⁵⁸A. A. Maradudin, P. Mazur, E. W. Montroll, and G. H. Weiss, *Rev. Mod. Phys.* **30**, 175 (1958).
- ⁵⁹H. J. Lipkin, *Ann. Phys. (N. Y.)* **23**, 28 (1963).
- ⁶⁰P. G. Dawber, and R. J. Elliott, *Proc. Roy. Soc. London Ser. A* **273**, 222 (1963).
- ⁶¹G. Weiss and A. Maradudin, *J. Phys. Chem. Solids* **7**, 327 (1958).